NATIONAL ADVISORY COMMITTEE FOR AERONAUTICS

TECHNICAL MEMORANDUM NO. 1159

WIND-TUNNEL MEASUREMENTS ON THE WING OF THE HENSCHEL MISSILE "ZITTERROCHEN"[1] IN SUBSONIC AND SUPERSONIC VELOCITIES*

By Kehl

Abstract: Supplementing the measured results previously reported, this investigation of three-component measurements on a wing model of the missile "ZR 2.0" was conducted in the subsonic wind tunnel (open-jet 215-millimeter diameter) and in the supersonic wind tunnel (open jet 110 by 130 millimeters) at the request of the Henschel Aircraft Works, Berlin.

Outline: I. Relations and Definitions

II. Description of Model and Measured Results

I. RELATIONS AND DEFINITIONS

A Lift, component of the air force perpendicular to the direction of flow, kilograms

W drag, component of the air forces in the direction of flow, kilograms

---

*"Windkanalmessungen am Flügel des Henschelgerätes 'Zitterrochen' bei Unter- und Überschallgeschwindigkeiten." Zentrale für wissenschaftliches Berichtswesen der Luftfahrtforschung des Generalluftzeugmeisters (ZWB) - Berlin-Adlershof, Untersuchungen und Mitteilungen Nr. 3161. Oct. 24, 1944.

[1]Literally "trembling ray."

M_o moment, referred to the center of the wing leading edge (tail loaded moment positive), meter-kilograms

F wing area, meters^2

b wing span, meters

l wing chord, meters

l_m mean wing chord, meters $\left(\frac{b}{\Lambda}\right)$

ρ air density (kg sec^2 m^{-4})

v stream velocity (m sec^{-1})

a sonic velocity (m sec^{-1})

α angle of attack, degrees

Λ wing aspect ratio $\left(\frac{b^2}{F}\right)$

M Mach number $\left(\frac{v}{a}\right)$

c_a lift coefficient $\left(\frac{A}{\frac{\rho}{2} v^2 F}\right)$

c_w drag coefficient $\left(\frac{W}{\frac{\rho}{2} v^2 F}\right)$

c_{m_o} moment coefficient $\left(\frac{M_o}{\frac{\rho}{2} v^2 F l_m}\right)$

II. DESCRIPTION OF MODEL AND MEASURED RESULTS

In figure 1 the wing under investigation with $\Lambda = 2$ is sketched. The contours are the biconvex profile formed by two circular arcs. The thickness ratio amounts to 6.3 percent. The wing was tested in two directions; these directions A and B are illustrated in figure 1.

The measurements in the subsonic wind tunnel (open-jet 215-millimeter diameter) at $M = 0.5$, 0.7, and 0.85

were taken, as were measurements in the supersonic wind tunnel (open jet 110 by 130 millimeters) at $M = 1.20$, 1.45, and 1.99. Angle of attack ranged from 0° to 10°. The polars and the moment-coefficient curves are given in figures 2 to 5.

For case A, a decrease in the drag was observed with increasing Mach number, just as was formerly noticed on the whole model (see UM 3122), which is traceable to laminar separation at the low Mach numbers. The Reynolds number based upon the mean chord l_m amounts to 3.2×10^5 at $M = 0.5$ and to 4.1×10^5 at $M = 0.85$. In contrast, the case B shows no Reynolds number or Mach number effect on $c_{w_{min}}$ over the same velocity range. In both cases, the lift coefficient increases with Mach number approximately as required by the Prandtl equation.

As was expected, at supersonic velocities the drag coefficient decreased with increasing Mach number at the low values of lift coefficient. Likewise, the lift coefficient decreased with increasing Mach number for a constant angle of attack.

The pressure point in supersonic as well as subsonic flow is independent of Mach number over the range of velocities investigated. In supersonic flow, however, the pressure point lies farther to the rear than in subsonic flow.

Translated by Chance Vought Aircraft Corporation

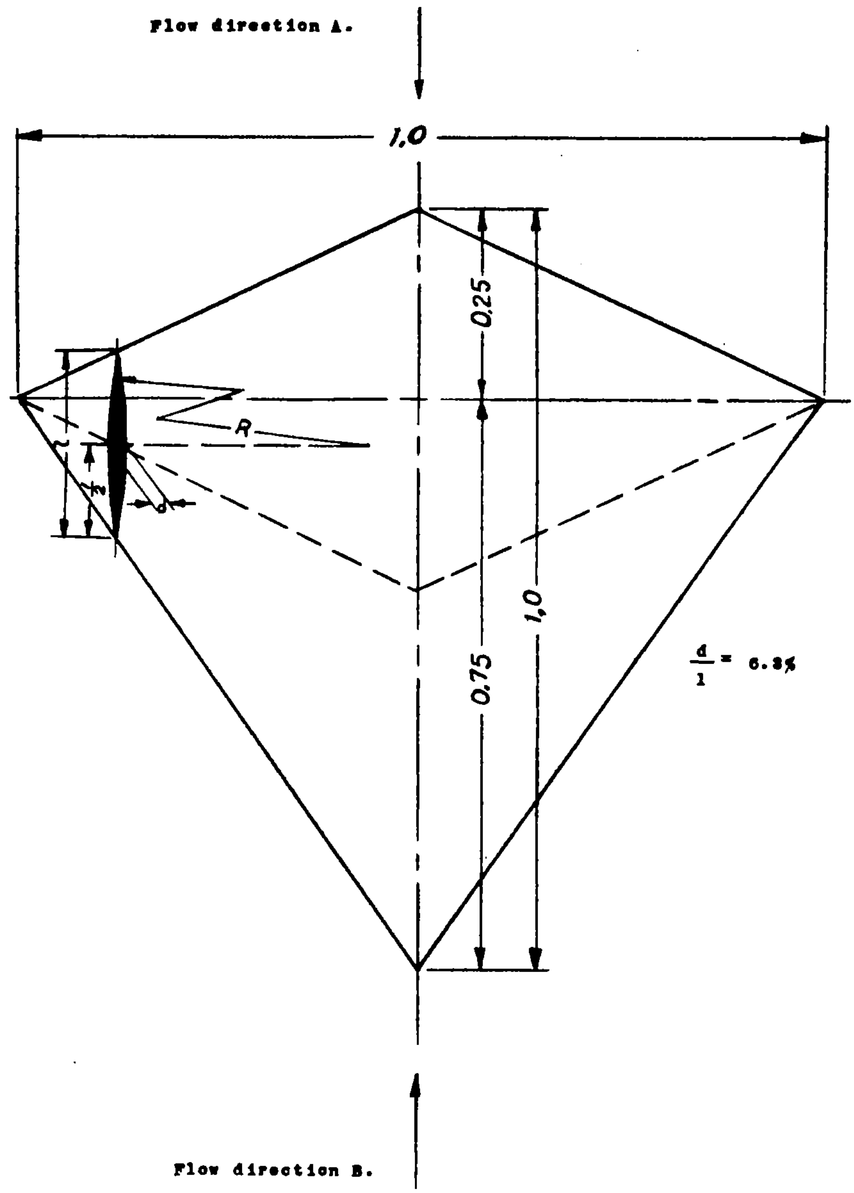

Figure 1.- Wing ZR 2.0; Λ = 2.0.

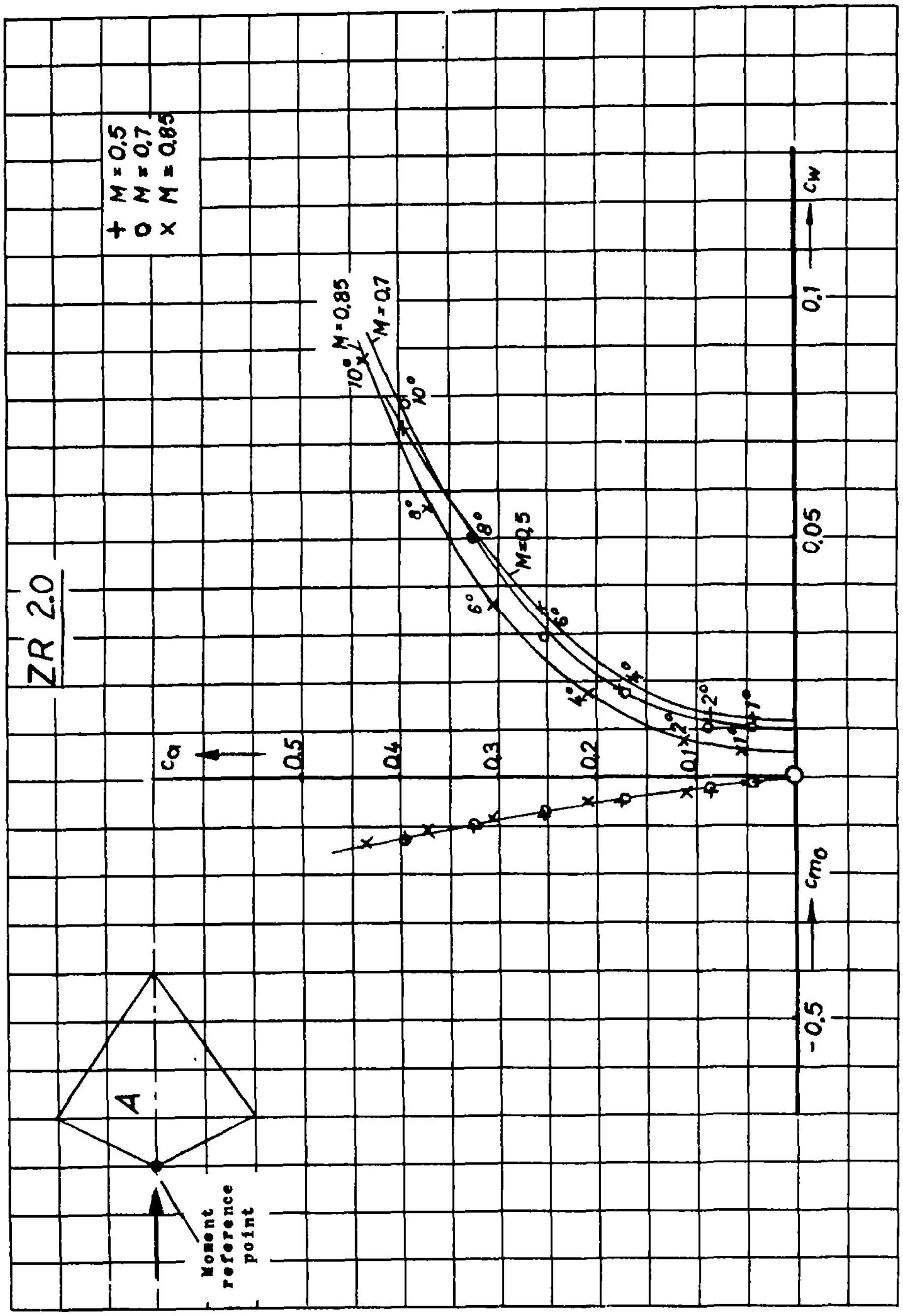
ZR 2.0
+ M = 0.5
o M = 0.7
× M = 0.85
M = 0.85
M = 0.7
M = 0.5
ca
cw
cmo
0.5
0.4
0.3
0.2
0.1
0.1
0.05
-0.5
A
Moment reference point

Figure 2.

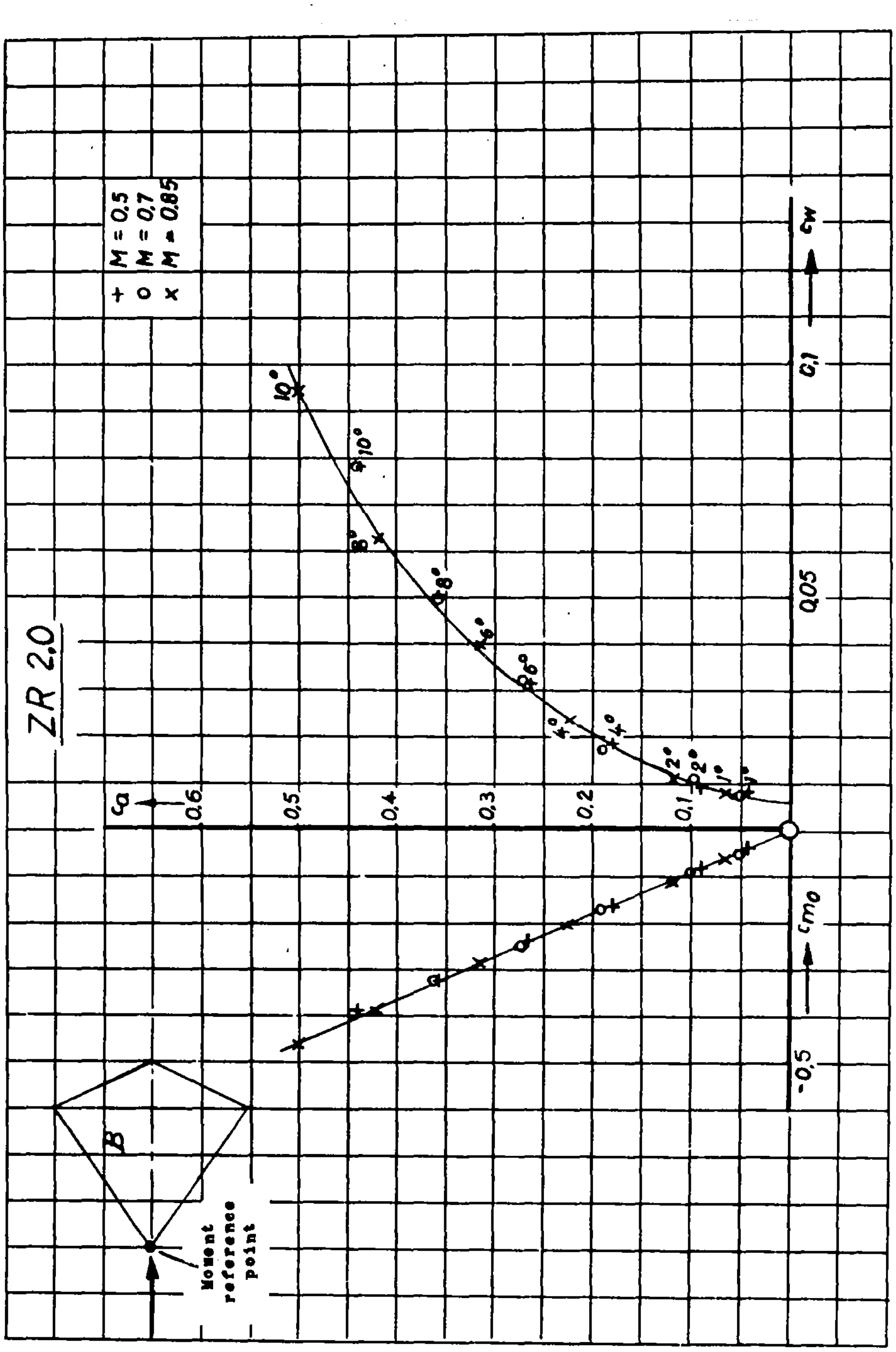
ZR 2,0
+ M = 0,5
o M = 0,7
x M = 0,85
c_a
c_w
c_{mo}
0,6
0,5
0,4
0,3
0,2
0,1
0,05
0,1
-0,5
B
Moment reference point

Figure 3.

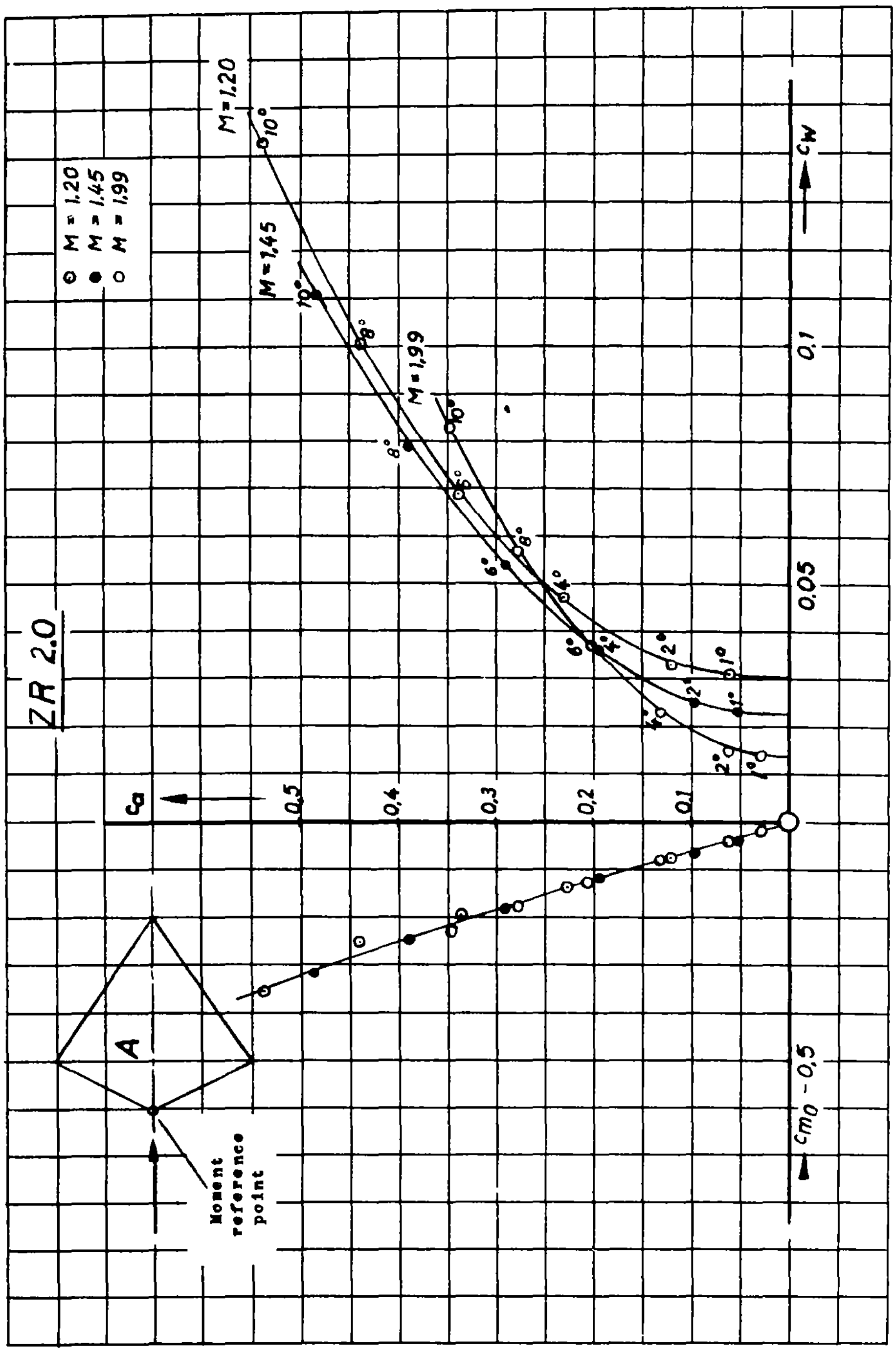

Figure 4.

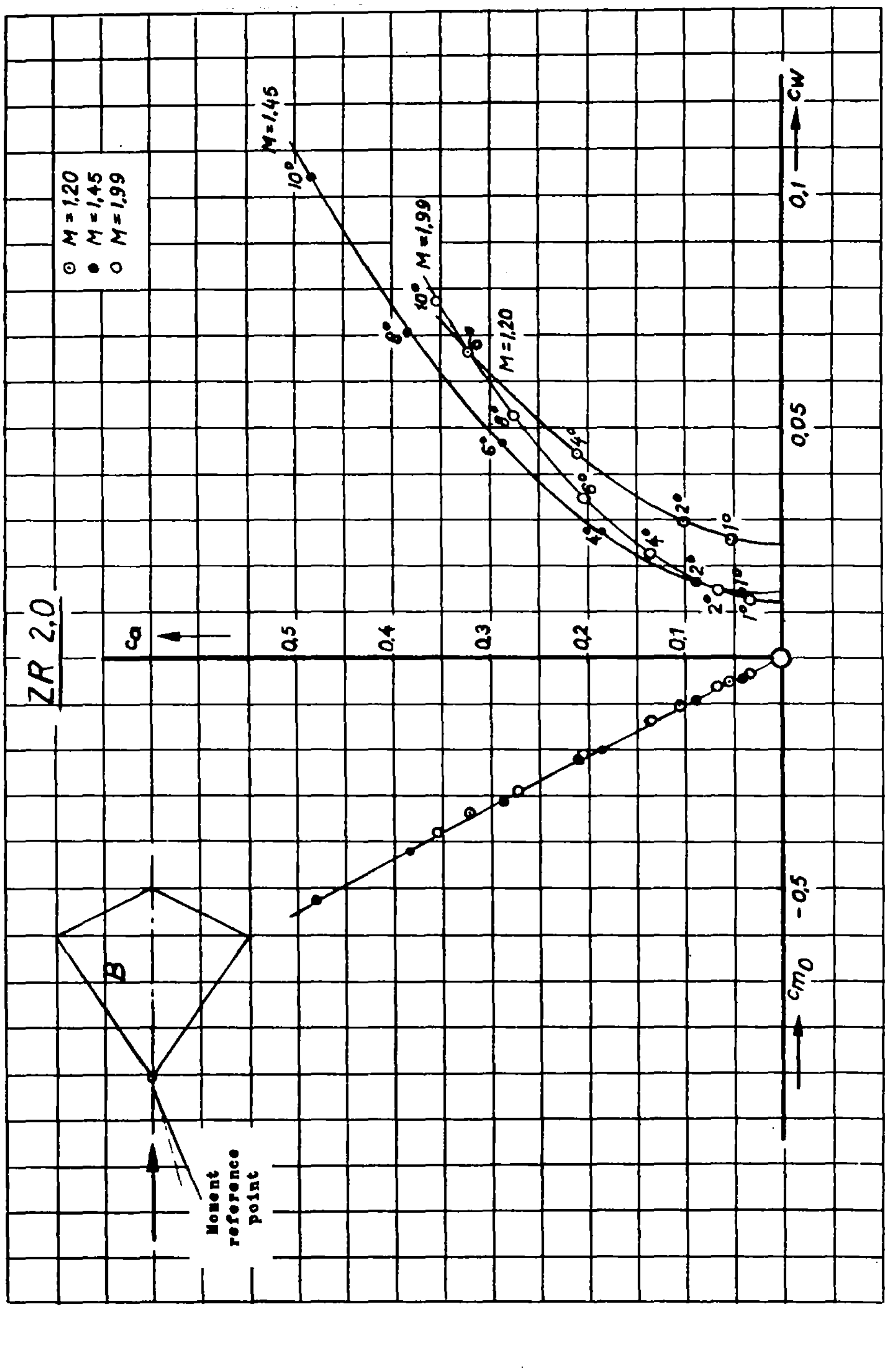
ZR 2,0
⊙ M = 1,20
● M = 1,45
○ M = 1,99
M = 1,45
M = 1,99
M = 1,20
ca
cw
cmo
0,5
0,4
0,3
0,2
0,1
0,05
0,1
-0,5
B
Moment reference point

Figure 5.